Soil deformation pattern in low-energy dynamic compaction

Modèle de déformation du sol au compactage dynamique à faible énergie

M. Hajialilue-Bonab & A.H. Rezaei
University of Tabriz, Tabriz, Iran

ABSTRACT

A physical modeling of low energy dynamic compaction (DC) on fine dry loose sand based on image processing was undertaken. The effective factors of DC and the deformation pattern of sand after tamper drops have been studied using image processing (PIV method). Having displacements of patches, the strains of elements formed of these patches were determined. The changes in relative density due to impacts, in different depths, were evaluated using total volumetric strains. A normalized relation between influence depth and DC parameters presented for low-energy DC design and prediction of influence depth of improvement. Also by derivation of crater depth versus drop number curves, the influence value of each impact in increase of improvement depth was defined.

RÉSUMÉ

Modélisation physique du Compactage Dynamique (CD) à faible énergie sur le sable lâche et sec, basé sur le traitement d'image a été entreprise. Les facteurs efficaces du CD et du modèle de déformation du sable après des frappes ont été étudiées en utilisant le traitement d'image (méthode de PIV). Ayant des mouvements de morceaux de sol à grains fins, la contrainte des éléments constitués de ces morceaux sont déterminée. Les changements de la densité relative due au compactage, dans différentes profondeurs, ont été évalués en utilisant des contraintes volumétriques totales. Une relation normalisée entre la profondeur influencée et les paramètres de CD a été présenté. Il peut servir pour la conception de compactage dynamique à faible énergie et la prévision de la profondeur influencée. En outre par dérivation de profondeur de cratère contre le nombre de frappe, la valeur d'influence de chaque impact dans l'augmentation de la profondeur d'amélioration a été définie.

Keywords : Dynamic Compaction, Image Processing, Soil Improvement

1 INTRODUCTION:

Dynamic compaction (DC) is among the most field proven and commonly used techniques, especially for the regions that the land has gained from the sea. This technique has been proven to be applicable to a wide range of soil types. The depth and degree of the ground improvement by using this technique are a function of the energy imparted to the soil by the falling mass. Mayne et al. (1984) reported a depth of improvement up to 33 m. It is not always necessary to achieve ground improvement to great depths: for example, when the ground to be modified consists of a layer of loose material with a depth of only a few meters, or when only a small increase in bearing capacity is required. In an attempt to provide a rapid, economic and efficient ground improvement system, this has led to the development of low-energy dynamic compaction

For many years as a soil improvement process, DC formalized in a simple manner By Menard & Broise (1975). The depth of influence d_{max} to impact energy for various soil types is given by:

$$d_{\max} = n\sqrt{W.H} \qquad [1]$$

Where W is the dropped weight in Tons, and H is the height of drop in meters. The value of empirical coefficient n ranges from 0.35 to 0.6 depends on soil type. Despite of extensive application of Eq.[1] in design of DC, this approach is an over-simplification of the problem and in practice the depth of compacted soil will be influenced by other factors such as the total applied energy, momentum, shape and base area of the tamper and grid spacing. Current practice for determination of optimum field operation parameters for DC technique relies mainly on field pilot tests and past experience based on case histories. Beside practical methods, application of physical and numerical models will be useful in investigation of compaction mechanism and wave propagation in soil. Laboratory dynamic compaction tests have been carried out by a number of researchers. Poran & Rodriguez (1992) introduced dimensionless relations to design of DC based on laboratory tests. Oshima and Takada studied the effect of the momentum of a tamper and presented some graphs for estimation of the improvement depth during dynamic compaction by using a variety of facts obtained from site tests and centrifuge model tests. Approximately, in all of these researches, value of strain, stress, penetration resistance or other parameters measure in few points into soil deposit by instrumentation. Because of limitation of number of measurement points no general displacement pattern of soil was presented.

In this research an attempt to study of effective factors of low-energy DC and deformation pattern of soil after compaction have been carried out using a physical modeling based on image processing. In the following details of tests and results has been represented.

2 CHARACTERISTICS OF PHYSICAL MODEL

A rigid wooden box with dimension of 700×470×830 mm has been used to undertake physical models of sand medium. A 20 mm thick transparent Perspex was erected in the front side of the box in order to monitoring displacement.

Proceedings of the 17th International Conference on Soil Mechanics and Geotechnical Engineering
M. Hamza et al. (Eds.)

doi:10.3233/978-1-60750-031-5-542

This study was done on dry fine sand prepared from north east of Tabriz (Ana Khatoun) in the north west of Iran. According to the unified soil classification system (USCS) this sand is poorly graded (SP). Table 1 represents the properties of this sand (ASTM [D854-92, D4254-91]).

Table 1. Mechanical properties of tested sand

G_s	C_u	C_c	D_{50}
2.632	2.58	1.18	0.84
D_{max} (mm)	D_{min} (mm)	$\gamma_{d\,max}$ (kN/m^3)	$\gamma_{d\,min}$ (kN/m^3)
2	0.25	17.29	14.90

A dry sand pluviation technique was used to prepare loose dry specimens with an initial depth of 50cm. In order to obtain homogeneous models in desired relative density a constant drop height of sand particles was obtained by lifting the container at a constant speed equal to the rate of increase in the thickness of the sand specimen. After sand raining, the average relative density of model was determinable for each test by measurement of weight of model and having box volume.

Tamping was executed by raising and dropping the steel tampers in semi-cylindrical section with known diameters and weights on the surface of sand deposit .Because of the axisymmetry, half of soil mass and tamper was modeled. Two 6.1 mm diameter holes made on the gravity center of each quadrant of tampers and also two 6 mm diameter cylindrical bar as the guides were used to impose exact location of drop.

3 DIGITAL PHOTOGRAPHY AND IMAGE PROCESSING

A texture-driven technique for non-contact measurement of soil deformation in physical models was presented by White et al 2002. Using PIV, the movement of a fine mesh of soil patches is measured to a high precision.

After each impact on model surface, a digital image was captured using a Canon G6 digital camera with an image resolution of 3072 x 2304 pixels. All controls such as focus, gain and shutter speed was adopted automatically. Two special projectors in both sides of camera in 45 degree angle and in the level higher than camera optical axis were set to eliminate optical effects of environment on the viewing window and avoid errors because of random variation of pixel intensities**.** The great number of measurements (approximately 1200 patches from soil plane by choose 72 pixel for patch size) make it possible to investigate the displacement and deformation of the soil precisely, which is one of unique benefits of PIV to instrumentation. Having obtained the displacement vector field, it can be evaluated the strains at different point.

3 METHODS OF THE TEST

After each impact on model surface, a digital image has been captured from the deformed soil mass and the frequent images have been processed and displacement vectors of each patch between each pair of images have been obtained. Resulting displacement vectors are in image space and measured displacement vectors in units of pixels converted to object-space measurement units (e.g. mm) using a constant image scale factor. The deformed soil behind Plexiglas and resulted displacement have been presented for a sample test in figure 1and 2. Having displacements of patches, the strain of elements formed of these patches can be determined. In our experimental models the plane strain condition can not be applied because the model is axisymmetric. In order to calculate the strain, the wedge shape elements were defined. Having displacements the area before each impact and after impact can be calculate.

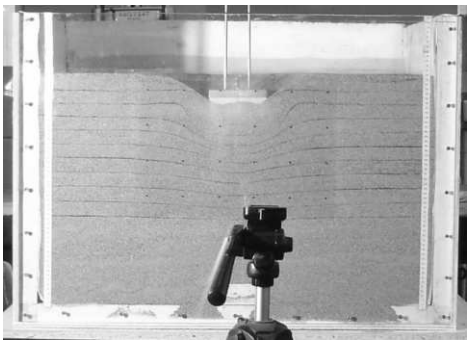

Figure 1. Soil condition after dynamic compaction

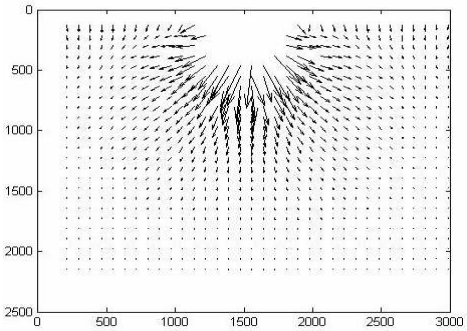

Figure 2. Displacement pattern after impact

Since the weight of elements is constant during test and initial volume and density of element are known, the change of elements density due to each impact can be determined .Knowing the density of element and having $\gamma_{d\,min}$ and $\gamma_{d\,max}$, the relative density of elements after each impact can be computed. This help to plot the contours of D_r in viewing area (Fig. 3). Figure 4 gives another results of this calculation in which the relative density of different depth under tamper centre for various number of drops are given.

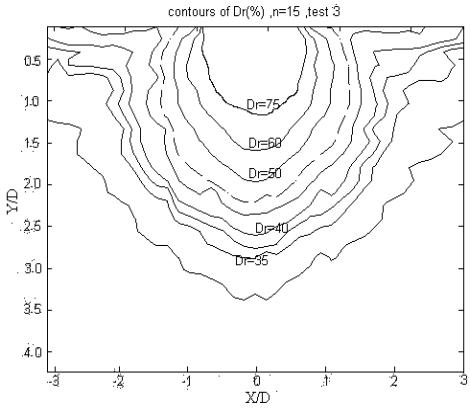

Figure 3. Distribution of relative densities variation in observed plane of soil

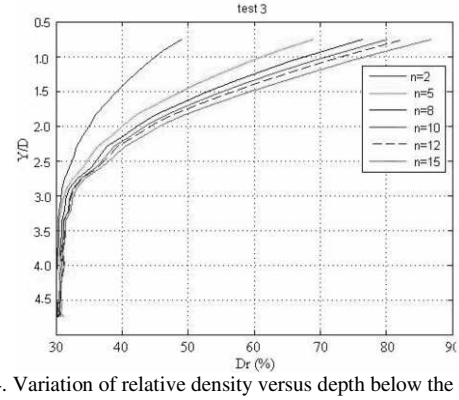

Figure 4. Variation of relative density versus depth below the center

4 TEST RESULTS

In this investigation, 13 tests with various values of affective factors on dynamic compaction were carried out. Table 2 gives the characteristics of tests and prepared models. Tests 4 and 5 have been performed with same properties in order to insure the reputability of the tests.

Table 2. Characteristics of tests

Test	Tamper weight (N)	Drop height (mm)	Tamper diameter (mm)	energy intensity ($kN.m/m^2$)	Momentum (N.m/s)
1	13.87	712.5	100	2.517	52.36
2	13.87	912.5	100	3.223	59.25
3	13.87	512.5	100	1.810	44.41
4	20.04	712.5	100	3.636	75.65
5	20.04	712.5	100	3.636	75.65
6	6.50	728	100	1.205	24.80
7	6.50	728	75	2.142	24.80
8	6.50	728	120	0.837	24.80
9	16.08	765	100	3.133	62.90
10	12.95	950	100	3.133	56.45
11	21.68	567.5	100	3.133	73.04
12	13.66	900	75	5.566	57.95
13	13.66	900	120	2.174	57.95

4.1 *Influences depth*

In this research the volumetric strain of 1.5% was chosen as criteria for influence depth. In order to evaluate the influence depth of each test the 1.5% volumetric strain contours for tests after each drops were plotted using PIV analysis. In order to reduction of scale effects, the method proposed by Poran et al. is applied. In the mentioned method, improvement depth (DI) is scaled to tamper diameter (D) and a normalized energy index, N.W.H/A.DI, is considered. In this phrase, N is the number of drops, W is the weight of the tamper in mega grams, A is the base area of the tamper in m^2 and H is drop height in meters. The above explained method is applied to all tests of this research and the result for the non- dimensional equation is shown in figure5 beside correlation coefficients. There is a linear relation between DI/D and N.W.H/A.DI in semi-logarithmic system. In other words, in a test when DC parameters are known, the influence depth could be estimated. The equation presented in this research is suitable for estimation of influence depth in low applied energy intensity dynamic compaction treatments.

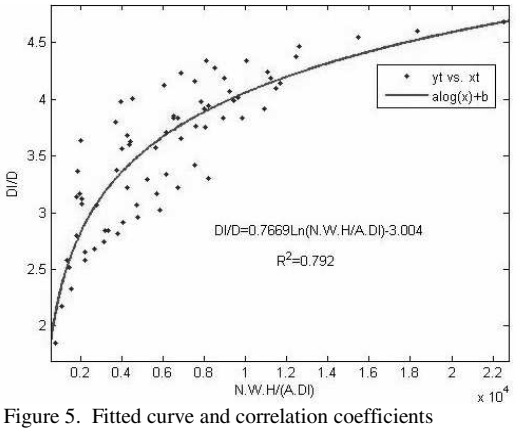

Figure 5. Fitted curve and correlation coefficients

4.2 *General pattern of soil deformation*

Having displacement vectors of soil patches it can be observed the soil deformation pattern and can study the effective parameters of DC. The deformation of different point of soil after each impact for all tests can be plotted. In figure 6 the general shape of occurred displacement after 10^{th} impact are shown for example. It can be observed that displacement of horizontal levels of soil mass in any depth has a bell- shape curve or Gaussian distribution curve.

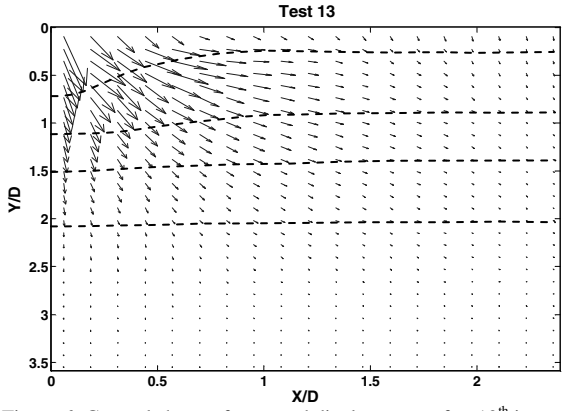

Figure 6. General shape of occurred displacement after 10^{th} impact

The direction of displacement vectors with respect to horizontal plane (angle θ) can be used as a criterion for compare deformation patterns in different point of soil media**.**

In order to compare the effect of applied energy for the same tamper area, the displacement vectors angle versus normalized distance from center for tests 13 and 8 after 12^{th} drop are shown in figure 7. It is observed that the values of angle of vectors in the same depth for test 13 (larger applied energy) are greater in comparison with test 8.

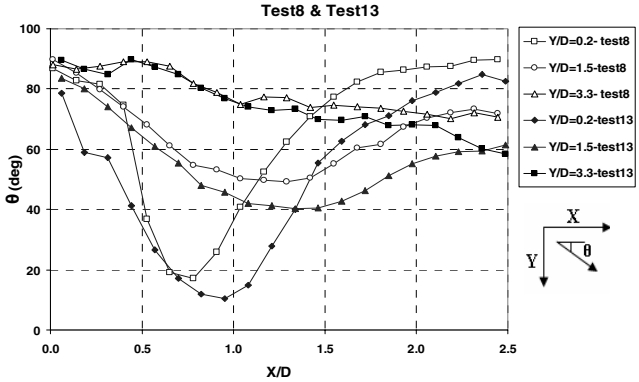

Figure 7. Angle of displacement vectors versus X/D curve for n=12.

4.3 *The crater properties*

The depth of crater with respect to drop number for tests 10, 12 and 13 are shown in figure 8 as an example of the measurements of crater depth. By derivation of crater depth versus drop number curves, the influence of each impact in increase of improvement depth was investigated. Figure 9 shows this curve for tests 13 as an example. It is found that after 8th drop the influence of impacts in improvement depth, was reduced and after 15th drop it is almost negligible. The main portion of improvement depth in granular soils can be obtained in the initial impacts and more impacts can just increase the density of improved ground.

4.4 *Efficiency of impact pressure*

In order to study the efficiency of impact pressure (W/A) in DC, three physical models were prepared (models 9, 10, 11). In these tests the applied energy (W.H) and the base area of tampers were similar. Figure 10 shows the contours of generated displacement in central plane after 12 drop into soil medium. It is found that for constant energy, with greater impact pressure a greater improvement and influence depth can be achieved in comparison with low impact pressure. It can be

concluded that the influence of tamper mass is greater than the drop height. In the other word the influence of momentum is greater than applied energy.

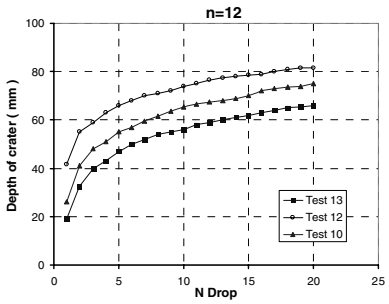

Figure 8. Depth of crater versus number of drop

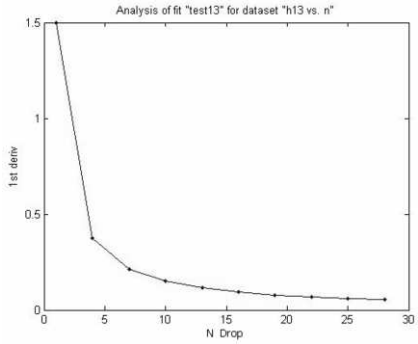

Figure 9. Derivation of crater depth versus drop number

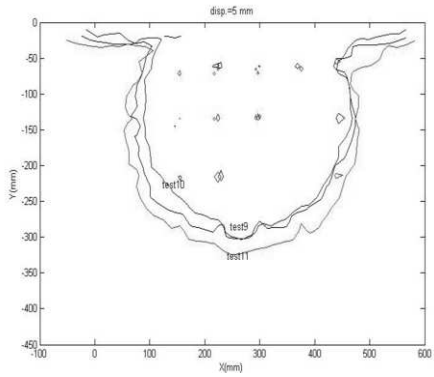

Figure 10. Contours of 5mm generated displacement in observed plane of soil

4.5 *Efficiency of tamper diameter*

Efficiency of tamper base area was investigated using the results of two series of tests 10, 12, 13 and 6, 7, 8. For each series same total energy were applied with different energy intensity per unit area. Figure 11 shows the contours of the 5mm displacement occurred after 12 drop for three tests 10, 12 and 13 for example. It is appear that there is no regular relation between tamper base area and influence depth.

In order to investigate closely this phenomena, the displacement filed of these tests in viewing plan were compared. It is observed that for higher energy intensity with same applied energy and momentum, larger displacements were occurred beneath tamper in the shallow depth comparing other tests that corresponds to larger depth of created crater (figure 8). It can be concluded when the area of tamper decrease, the energy intensity increase and the most portion of applied energy was consumed to create large deformations in soil mass beneath the tamper with decreased influence radius. Decrease of tamper base area cause increase in stress and degree of improvement to depth about 1.2-1.4 times the diameter of tamper and the most portion of applied energy consume to cause large deformations in soil mass.

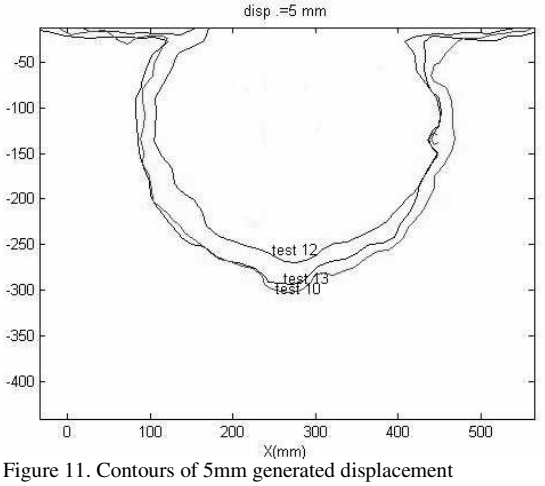

Figure 11. Contours of 5mm generated displacement

5 CONCLUSION

The deformation field of soil mass after dynamic compaction was investigated and generated strain and change in relative density due to impacts, in different depths, are evaluated.

It is found that the main portion of improvement depth in granular soils can be obtained in the initial impacts and more impacts just increase the density of improved ground.

For the same initial relative density, the depths of the crater in all tests increase with increase in drop height.

For constant energy, the DC with greater impact pressure cause greater influence depth and improvement in comparison with low impact pressure. In the other word the influence of momentum is greater than applied energy.

Decrease of tamper base area cause increase in stress and degree of improvement to depth about 1.2-1.4 times the diameter of tamper and the most portion of applied energy consume to cause large deformations in soil mass.

REFERENCES

Lukas,R.G. 1995. Dynamic Compaction. Geotechnical Engineering Circular No.1, Publication No .FHW A-SA-95-037 , Federal Highway Administration, Washington , DC, 97pp

Mayne, P.W, Jones, J.S. & E'Dinas, D. C. 1984. Ground response to dynamic compaction. Journal of Geotechnical Engineering, ASCE 110, No. GT6, 757-773.

Menard, L. & Broise,Y. 1975.Theoretical and Practical Aspects of Dynamic Consolidation. Geotechnique, Vol. 25, No. 1, pp. 3-18.

Merrifield, C.M. & Davies, M.C.R. 2000. A study of low-energy dynamic compaction: field trials and centrifuge modeling. Geotechnique 50, No. 6, 675-681.

Poran, C.J. & Rodriguez, J.A. 1992.Design of dynamic compaction. Canadian Geotechnical Journal. Vol.29, No.1, pp.796-802

Poran,C.J., Rodriguez .J.A. & Heh, K.S. 1992.Impact behavior of sand. soils and foundations ,Vol.32 ,No4, December pp .81-92

White, D.J., Take, W.A. & Bolton, M.D. 2003. Soil deformation measurement using particle image velocimetry (PIV) and photogrammetry. Géotechnique 53,No. 7,pp 619-631.

White, D.J., Take, W.A. & Bolton, M.D. 2001 .Measuring soil deformation in geotechnical models using digital images and PIV analysis. Proc. 10th Int. Conf. on Computer Methods and Advances in Geomechanics. Tucson, Arizona. pub. Balkema, Rotterdam pp 997-1002.

Oshima, A. & Takada,N. 1994. Effect of ram momentum on compaction by heavy tamping . International Conference on Soil Mechanics and Foundation Engineering ,13(3)pp1141-1144.

Oshima, A. & Takada,N. 1998. Evaluation of compacted area of heavy tamping by cone point resistance. Balkema, Rotterdam, ISBN 90 5410 9866.